

# Experimental study of the interaction between localized and propagating surface plasmons

Yizhuo Chu and Kenneth B. Crozier\*

School of Engineering and Applied Sciences, Harvard University, Cambridge, Massachusetts 02138, USA

\*Corresponding author: kcrozier@seas.harvard.edu

Received August 18, 2008; revised November 6, 2008; accepted November 14, 2008;  
posted December 10, 2008 (Doc. ID 100254); published January 22, 2009

The interaction between localized and propagating surface plasmons is investigated in a structure consisting of a two-dimensional periodic gold nanoparticle array, an SiO<sub>2</sub> spacer, and a gold film. The resonance wavelengths of the two types of surface plasmons supported by the structure are tailored by changing the gold nanoparticle size and the array period. An anticrossing of the resonance positions is observed in the reflection spectra, demonstrating the strong coupling between localized and propagating surface plasmons.

© 2009 Optical Society of America

OCIS codes: 240.6680, 250.5403.

Surface plasmons (SPs) are a collective oscillation of electrons at the boundaries between materials and are often categorized into two classes: propagating surface plasmons (PSPs) and localized surface plasmons (LSPs) [1]. PSPs are propagating electromagnetic waves bound to the interfaces between metals and dielectrics. They can be excited on a metal surface by prism coupling or by grating coupling over a large range of frequencies. LSPs, on the other hand, are nonpropagating excitations of the electrons in metal nanoparticles that are much smaller than the incident wavelength. The resonance wavelength of LSP is dependent on the size, shape, and dielectric function of the nanoparticle as well as the dielectric environment [2]. Both types of SP have attracted a lot of interest owing to their great potential for applications, such as surface-enhanced Raman scattering (SERS) and biosensors. It is therefore natural to consider how LSPs and PSPs interact, as structures combining both phenomena could offer favorable properties. Holland and Hall [3] observed a dipole–surface interaction by measuring the shift of the LSP resonance when randomly arranged silver nanoparticles were placed near a silver film. Stuart and Hall [4] pointed out that, in the same structure as that of [3], the PSP excited on the silver film enhanced a dipole–dipole interaction between individual nanoparticles. Cesario *et al.* [5] reported multiple resonance modes in the extinction spectra resulting from the coupling between LSP and PSP in a hybrid structure that combined a two-dimensional gold nanoparticle array and a thin gold film. Recently, theoretical studies have predicted that strong coupling between LSPs and PSPs occurs when their resonance frequencies are approximately equal [6,7].

In this Letter, we investigate the LSP–PSP interaction numerically and experimentally, using a structure combining a gold nanoparticle array with a gold film. A strong coupling between LSP and PSP is observed, as indicated by an anticrossing behavior of the resonance positions in the reflection spectra.

The geometry of the sample is shown in Fig. 1(a). A 100-nm-thick gold film is deposited on an indium–tin–oxide coated glass substrate by thermal evaporation with a 5-nm-thick chromium film used as an ad-

hesion layer. A 20-nm-thick SiO<sub>2</sub> spacer is deposited on the top of the gold film by plasma-enhanced chemical-vapor disposition. Finally, a two-dimensional gold nanoparticle array is fabricated by *e*-beam lithography and lift-off on top of the SiO<sub>2</sub> spacer, yielding the structure shown in Fig. 1(b). The gold nanoparticle arrays are square lattices (130 μm × 130 μm) of gold disks with periods varying from 620 to 880 nm. The diameters of the gold disks vary from 100 to 170 nm. The gold disks are 40 nm thick.

To understand the optical properties of this structure, we use the finite-difference time domain (FDTD) method to calculate the near-field intensity spectra. The side view of the structure that is modeled in the simulations is shown in the inset of Fig.

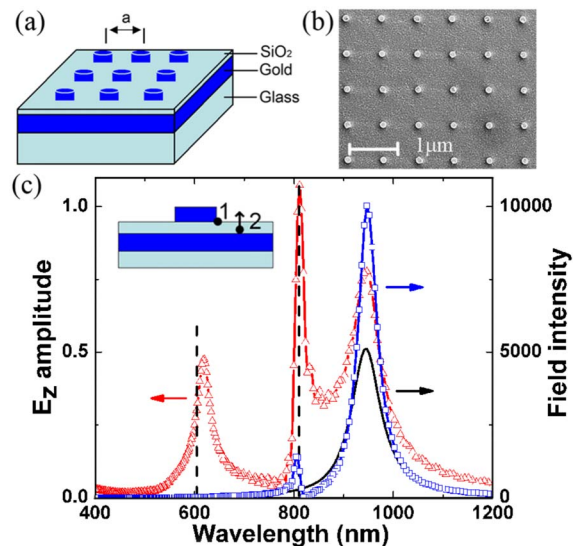


Fig. 1. (Color online) (a) Sketch of the structure's configuration. (b) Scanning electron micrographs of the gold disk array on the SiO<sub>2</sub> spacer and the gold film. (c) Near-field spectra of an isolated disk and a disk array ( $a=780$  nm). Black solid line, near-field intensity at position 1 for an isolated disk. Blue square, near-field intensity at position 1 for the gold disk array case. Red triangle,  $E_z$  amplitude at position 2 for the gold disk array case. Dashed curves, resonance wavelengths of the (1,1) and (1,0) PSP modes. Inset, side view of the structure.

1(c). The indexes of the glass substrate and the SiO<sub>2</sub> spacer are 1.517 and 1.46, respectively. The dielectric permittivity of gold used in the calculations is described by the Lorentz–Drude model, whose experimentally determined parameters are taken from [8]. The structure is excited by a linearly polarized plane wave from the top at normal incidence. Since the enhanced electromagnetic field of the LSP on a gold disk is mainly confined in a small area near the gold disk [9], we monitor the field intensity ( $E^2$ ) at the edge of the gold disk on the bottom surface [position 1 in the inset of Fig. 1(c)] to measure the LSP on the gold disk. In the nanoparticle array case, the periodic array provides an additional momentum  $G = (2\pi/a)\sqrt{p^2+q^2}$ , where  $a$  is the grating constant and  $p$  and  $q$  are integers, to couple the incident light into the PSP on the gold film. The distribution of surface charges arising from the grating induced PSP reaches a maximum at a quarter period away from the center of the gold disk [position 2 in the inset of Fig. 1(c)] [7]. Therefore, we monitor the amplitude of  $E_z$  at position 2 to measure the PSP on the gold film. In Fig. 1(c), we plot the near-field spectra as a function of wavelength for an isolated gold disk and for an array of grating constant of 780 nm. The gold disks are 150 nm in diameter and 40 nm thick. All the spectra are normalized by the corresponding spectra of incident light. The isolated gold disk on the SiO<sub>2</sub> spacer and gold film has a single resonance at  $\lambda_0 = 948$  nm [black solid curve in Fig. 1(c)] that is redshifted from the resonance of the same isolated gold disk on a glass substrate (746 nm, not shown). This strong redshift is due to the near-field interaction between the gold disk and its image [3,10]. In the gold disk array case, as discussed above, PSPs on the gold film are induced by the periodic array. The decay length of the PSPs in gold with air as the top half space can be expressed as  $l = (c/\omega)\sqrt{(\epsilon_m + \epsilon_i)/\epsilon_m}$ , where  $\epsilon_m$  and  $\epsilon_i$  are the permittivities of gold and air, respectively [11]. The decay length is  $\sim 42$  nm at 600 nm. For a 100 nm gold film, the PSPs on the two surfaces are decoupled. Here we only consider the PSPs on the top surface of the gold film. To calculate the theoretical frequencies of the PSP modes, we calculate the dispersion relation for PSPs for a structure consisting of a gold half space, an SiO<sub>2</sub> layer (20 nm thick), and a vacuum half space [1]. As discussed, the grating provides an additional momentum  $G = (2\pi/a)\sqrt{p^2+q^2}$  to couple into the PSP modes. From the dispersion relation, we find that the  $(p,q)=(1,0)$  and  $(1,1)$  PSP modes are coupled with free-space wavelengths of  $\lambda_0=810$  and 605 nm, respectively, for a period of  $a=780$  nm [dashed curves in Fig. 1(c)]. Compared with the isolated disk case, the near-field intensity spectrum of the disk array has an additional resonance at 807 nm [blue square curve, Fig. 1(c)], which is close to the wavelength of the  $(1,0)$  PSP mode from theory. In the spectrum of  $E_z$  amplitude on the gold film [red triangle curve, Fig. 1(c)], three resonances can be seen. The first two resonances at 811 and 617 nm correspond to the  $(1,0)$  and  $(1,1)$  modes of the PSP on the gold film, respectively.

The third resonance occurs at a very similar wavelength to that of the isolated disk and corresponds to the LSP of the gold disks. It can be seen that the near-field enhancement at resonance for an isolated gold disk on the SiO<sub>2</sub> spacer and gold film is  $\sim 5000$ , which is much higher than the peak intensity enhancement of the same gold disk on a glass substrate ( $\sim 300$ , not shown). The interaction of the gold disk and its image enhances the local-field intensity. The near-field intensity for the array of gold disks on the SiO<sub>2</sub> spacer and gold film at the LSP resonance is about twice as large as that of the isolated disk on the SiO<sub>2</sub> spacer and gold film, indicating that the gold film PSP enhances the LSP in the gold disks further.

To investigate the coupling of localized and propagating PSPs, in both theory and experiment, we tune the resonance wavelengths of the PSP mode on the gold film by changing the period of the array, with the size of the gold disks constant (diameter 120 nm and thickness 40 nm). In Fig. 2(a), the calculated resonance wavelengths of the  $(1,0)$  PSP mode and the LSP are plotted as a function of period (dots). The dashed line indicates the free wavelengths for coupling to the  $(1,0)$  PSP modes calculated by theory and the dotted curve indicates the free space resonance wavelengths for coupling to the LSP of an isolated disk obtained from FDTD simulations. An anticrossing behavior can be seen when the resonance

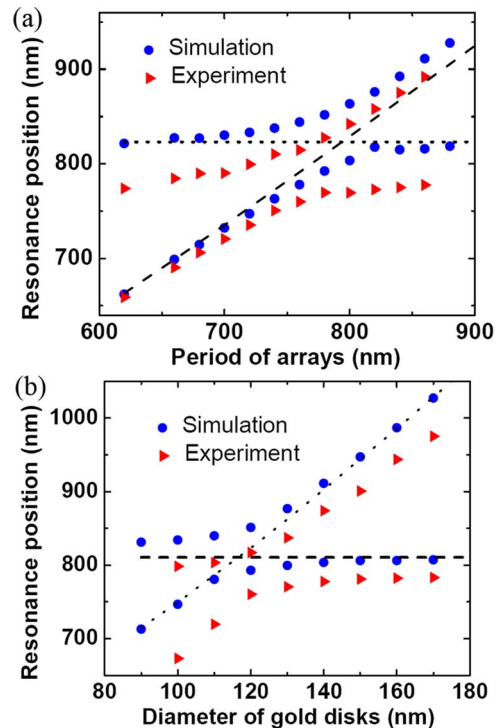


Fig. 2. (Color online) Resonance positions of the LSP and the  $(1,0)$  PSP mode (a) as a function of the grating period and (b) as a function of the diameter of the gold disk. Dots, simulation results of the near-field intensity at position 1. Triangles, experimental results obtained by reflection measurements. Dashed curves, resonance wavelengths of the  $(1,0)$  PSP mode (calculated by theory). Dotted curves, resonance wavelengths of isolated gold disks on the SiO<sub>2</sub> spacer and the gold film (calculated by simulations).

wavelengths of the isolated gold disk and the PSP are approximately equal, at a period of 780 nm. Similarly, we tune the free-space resonance wavelengths for coupling to the LSP on the gold disk by changing the size of the gold disk while keeping the period constant at 780 nm. The results are shown in Fig. 2(b). A clear anticrossing is seen at a disk diameter of  $\sim 120$  nm. The anticrossing implies strong coupling between PSPs and LSPs.

To observe this strong coupling experimentally, we carry out reflection measurements on fabricated devices. The setup is shown in Fig. 3(a). The sample is illuminated at normal incidence by a collimated and polarized beam through a beam splitter. The reflected light is collected by a long working distance microscope objective and coupled into a spectrometer. An iris placed at the image plane of the objective ensures that only the light reflected by the array is detected. The reflection spectra are normalized by the spectrum of a region of the sample away from the gold disk array, i.e., consisting of the  $\text{SiO}_2$  spacer on gold. Measured and FDTD-calculated spectra of arrays of a 780 nm period with varied gold disk sizes are shown in Figs. 3(b) and 3(c). Good agreement can be seen in the comparison between the experimental results and the simulations. The blueshift of the resonances

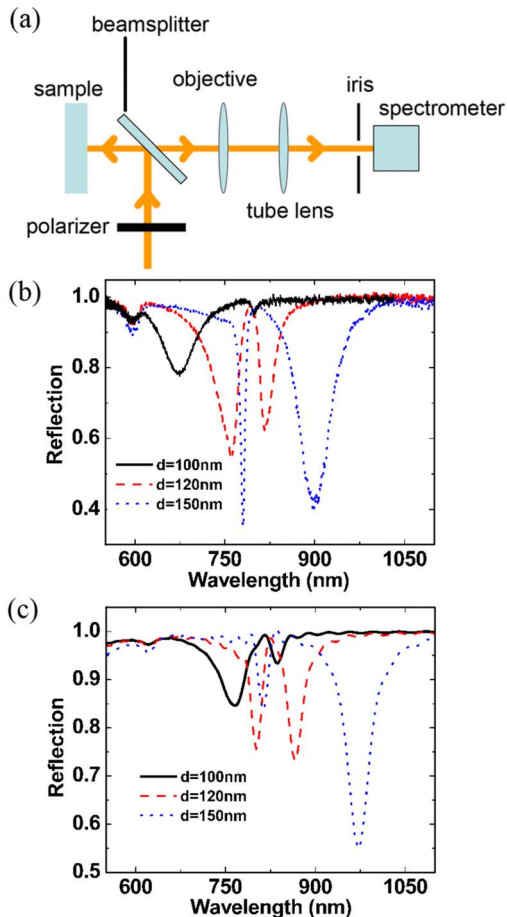


Fig. 3. (Color online) (a) Reflection measurement setup. (b) Measured and (c) calculated reflection spectra. Grating constant  $a=780$  nm, disk diameter  $d=100$  nm (solid),  $d=120$  nm (dashed), and  $d=150$  nm (dotted); disk thickness = 40 nm.

in the experimental spectra with respect to the simulated spectra could be due to the fabrication imperfection and/or differences in the dielectric constants of gold and  $\text{SiO}_2$  between simulation and experiment. The resonance at 595 nm in the experimental spectra is independent on the size of the gold disk, corresponding to the (1,1) PSP mode. In the spectrum of the sample consisting of 100 nm diameter gold disks [solid curve in Fig. 3(b)], the broad resonance at 672 nm is attributed to the resonance of LSP on the gold disks, and the relatively sharp resonance at 791 nm is attributed to the (1,0) PSP mode on the gold film. As the gold disk diameter increases, the resonance of the LSP moves to a longer wavelength and interacts with the (1,0) PSP mode. When the diameter of the gold disk is 120 nm [dashed curve in Fig. 3(b)], the resonances of the LSP and (1,0) PSP mode exhibit a repulsion behavior. For the spectrum of 150 nm in diameter [dotted curve in Fig. 3(b)], the LSP resonance occurs at  $\lambda=899$  nm, which is a longer wavelength than the (1,0) PSP mode ( $\lambda_0=810$  nm). The resonance wavelengths of the LSP and (1,0) PSP mode are plotted in Figs. 2(a) and 2(b) as red triangles. The experimental results clearly indicate the anticrossing behavior predicted by simulations, demonstrating the strong coupling between the LSP on the gold disks and the PSP on the gold film.

In summary, we study the interaction of gold nanoparticle arrays with a gold film that is in close proximity to the arrays. An anticrossing behavior of the resonance positions in the reflection spectra indicates a strong coupling between the LSP on the gold nanoparticles and the PSP on the gold film. The large near-field enhancement could make this structure useful for SERS and biosensors.

The authors acknowledge support from the Defense Advanced Research Projects Agency (DARPA) and the National Science Foundation (NSF). Fabrication work was carried out at the Harvard Center for Nanoscale Systems, which is supported by the NSF.

## References

1. S. A. Maier, *Plasmonics: Fundamentals and Applications* (Springer, 2007).
2. K. L. Kelly, E. Coronado, L. L. Zhao, and G. C. Schatz, *J. Phys. Chem. B* **107**, 668 (2003).
3. W. R. Holland and D. G. Hall, *Phys. Rev. Lett.* **52**, 1041 (1984).
4. H. R. Stuart and D. G. Hall, *Phys. Rev. Lett.* **80**, 5663 (1998).
5. J. Cesario, R. Quidant, G. Badenes, and S. Enoch, *Opt. Lett.* **30**, 3404 (2005).
6. N. Papanikolaou, *Phys. Rev. B* **75**, 235426 (2007).
7. A. Ghoshal and P. G. Kik, *J. Appl. Phys.* **103**, 113111 (2008).
8. A. D. Rakic, A. B. Djuricic, J. M. Elazar, and M. L. Majewski, *Appl. Opt.* **37**, 5271 (1998).
9. S. Zou and G. C. Schatz, *Chem. Phys. Lett.* **403**, 62 (2005).
10. P. Nordlander and E. Prodan, *Nano Lett.* **4**, 2209 (2004).
11. I. Puscasu, M. Pralle, M. McNeal, J. Daly, A. Greenwald, E. Johnson, R. Biswas, and C. G. Ding, *J. Appl. Phys.* **98**, 013531 (2005).